2018

Simulation of Seasonal Performance of a Membrane Heat Pump System in Different Climate Regions

Ahmad A. Bukshaisha
Oregon State University, United States of America, bukshaia@oregonstate.edu

Brian M. Fronk
Oregon State University, United States of America, brian.fronk@oregonstate.edu

Simulation of Seasonal Performance of a Membrane Heat Pump System in Different Climate Regions

Ahmad A. BUKSHAISHA[1], Brian M. FRONK[1]*

School of Mechanical, Industrial and Manufacturing Engineering
Oregon State University
Corvallis, OR, United States
541-737-3952, brian.fronk@oregonstate.edu

* Corresponding Author

ABSTRACT

Membrane based heat pumps systems have attracted the attention of many research groups as a potentially more environmentally friendly alternative to vapor compression systems that are being used for space cooling in 90% of the buildings in the United States. Several prototypes systems have been developed, with reported claims of EER of 26. However, no detailed analysis are publically available which demonstrates the capability of these systems in different climate zones. In this work, a full thermodynamic cycle model of a representative membrane heat pump system is developed and heat and mass transfer components were sized to provide 3 tons of cooling at nominal rating conditions. The main results were that the membrane heat pump system had an EER of 16-20 which is lower than some literature reported values. However, these systems had higher performance results than the conventional vapor compression system and performed well in the 6 different climate zones investigated.

1. INTRODUCTION

Heating, ventilation and air conditioning (HVAC) consumes 48% of the total energy in buildings in the United States, with 12.3% dedicated to space cooling (EIA, 2013). Vapor compression systems are used for space cooling in 90% of the buildings in the United States. A typical vapor compression heat pump relies on an evaporating and condensing fluid to transfer energy. The refrigerant is evaporated at a low pressure (removing heat from a conditioned space), and compressed to a high pressure where it is condensed, rejecting heat from the system. The fluid is then expanded to a lower pressure and the cycle repeats. This basic cycle has been in use for over one hundred years, yielding very reliable, efficient equipment. However, the work of compression is high, and the working fluids are often not environmentally friendly. Common refrigerants such as R-134a and R-410A are in the process of being phased out due to their high global warming potential. Thus, there has been significant interest in investigation non-vapor compression technology for cooling. One of the promising technologies identified by the United States Department of Energy (DOE) is the use of membrane based systems capable of transferring sensible and latent energy (Goetzler, Zogg, Young, & Johnson, 2014a). An example of a potential system configuration is shown in Figure 1, as reported in Goetzler et al. (2014b) and based on research conducted by DAIS Analytic.

The system couples a membrane vacuum dehumidification system with a membrane based indirect evaporative cooler. A vacuum pump creates a low vapor pressure to remove moisture from the supply air and from the indirect evaporative cooler loop, as shown. Then the vacuum pump discharges the water vapor to a third membrane module which transfer moisture to the ambient air. Therefore, the vacuum pump needs to compress the water vapor to the ambient water vapor partial pressure and not the absolute, hence reducing the compression ratio from ~100 to approximately 3-5. High energy efficiency ratio (EER) of this and similar membrane based cycles have been reported (Goetzler et al., 2014b), however, there is no detailed published performance data in the open literature. Thus, the objective of this work is to develop a simulation model of this membrane heat pump concept shown in Figure 1 and then predict seasonal performance in different climate regions within the United States. This is done by developing a full thermodynamic cycle model of the system and then sizing the heat and mass transfer components to provide 3 tons of cooling at nominal rating conditions for residential buildings. Energy performance ratings such as coefficient of performance (COP), and EER, as well as other utility parameters electricity cost will be evaluated

for different geographic locations. These results are then compared to conventional, high efficiency vapor compression systems.

2. MODEL DEVELOPMENT

2.1 Approach

To simulate performance of the system, an initial thermodynamic state point model was developed in *Engineering Equation Solver* (EES) (Klein, 2017) for a 3 ton cooling capacity and other assumed parameters at a nominal rating condition. Using this model, the physical size of the heat and mass exchangers and vacuum pump power at the nominal condition were determined. These values were then used as inputs into a more detailed physical model, which enabled the performance of the heat pump to be simulated under varying ambient conditions in different climate regions. The results of this model were compared to the seasonal performance of a representative vapor compression system.

2.2 Description of the Modeled System

The membrane heat pump system investigated in this paper is shown in Figure 1. Starting at state point 1 in Figure 1, hot humid return air enters the membrane dehumidifier. The vacuum pump creates the required differential pressure difference which extracts the moisture from the air through the selective membrane resulting in latent heat removal. Then, the warm, dry air passes through the chilled water coils, removing sensible heat and cooling the air down to the design supply temperature before entering the conditioned space (state point 3). The sensible cooling load is rejected through an evaporative cooling process take place at the membrane evaporative cooler, where water vapor from the circulating water loop is extracted by the vacuum pump (state 4 to 5) to maintain the cycle running at cool temperatures. The water vapor extracted from both the membrane dehumidifier and membrane evaporative cooler is rejected to the ambient through a third selective membrane humidification process by compressing the water vapor to a slightly higher pressure than the ambient partial vapor pressure. Finally, makeup water is added to the circulating coolant loop (state 13). The cooling process in this membrane heat pump system does not use any working fluid other than water, eliminating the use of high global warming potential working fluids. Furthermore, it decouples latent and sensible heat removal which opens up the possibility of novel control strategy of controlling the indoor temperature by controlling the dry-bulb and wet-bulb temperature separately.

2.3 State Point Simulation Model

The initial state point model was developed in EES to provide 3 tons of cooling at the ASHRAE residential rating conditions (ASHRAE, 2017) and the other assumed parameters shown in Table 1. In addition, it was assumed that the system operated at steady state and that pressure drop through each component was negligible. The goal from this model is to predict the required overall heat and mass transfer coefficients for each component, the vacuum pump power, and the required indoor air volumetric flow rate to provide 3 tons of cooling and a 12.78°C (55°F) supply air temperature.

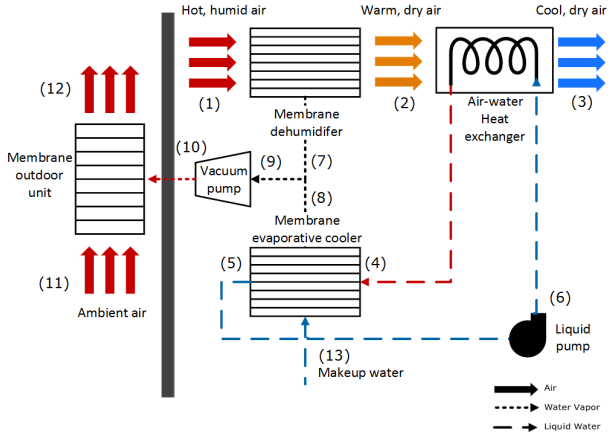

Figure 1: Schematic of membrane heat pump system

Table 1: Design conditions set for the membrane heat pump systems

Description	Value	Unit
Total cooling load	3	Tons
Indoor return air dry-bulb	26.7	°C
Indoor return air wet-bulb	19.4	°C
Design supplied air temperature	12.78	°C
Air flow into outdoor unit	1350	ft^3min^{-1}
Dehumidifier effectiveness	0.7	-
Vacuum pump isentropic efficiency	0.75	-
Liquid pump isentropic efficiency	0.90	-
Circulating water loop mass flowrate	0.2	kg s^{-1}
Makeup water temperature	15	°C

State point 1 is the return air from the conditioned space. Pressure, temperature and relative humidity are known from the rating conditions, thus, all thermodynamic properties including humidity ratio is fully defined. The humidity ratio at the outlet of the membrane humidifier is determined from the assumed effectiveness, as shown in Equation (1). The pressure is assumed to remain constant in the air stream. ft^3min^{-1}

$$\omega_2 = \omega_1 - \epsilon_{dehumidifier}\omega_1 \quad (1)$$

The water vapor is removed to state point 7. Here, it is assumed that the water vapor temperature is equal to the humid air temperature at state 1, as the dehumidification process is approximately isothermal. The other property is the pressure, which must to be less than the partial vapor pressure at state point 2. The simulation model defines the pressure at state 7 using the variable *Z,* as shown in Equation (2). A higher value of Z requires a high compression ratio but smaller heat and mass exchanger to achieve the same moisture removal. On the other hand, a smaller value yields a bigger heat and mass exchanger (smaller driving pressure differential), but decreases the required pressure ratio for the vacuum pump, increasing the COP. The assumed value of Z is 0.1, chosen based on a tradeoff analysis between COP and size of the heat and mass exchanger. This assumption is removed in the physical model, as the vacuum pump power and heat and mass exchanger size are specified, as described below.

$$P_7 = P_{v2} - ZPv_2 \quad (2)$$

The enthalpy at state 2 is calculated from an energy balance on the dehumidifier, as shown in Equation (3) below. The mass flowrate is calculated from Equation (4) where h_3 is evaluated using the design supply air temperature and ambient pressure, and ω_3 which is equal to ω_2. The specific enthalpies in Equations 3 and 4 are evaluated on a kJ per kg of dry air basis, by convention.

$$\dot{m}_a h_1 = \dot{m}_a[h_2 + (\omega_1 - \omega_2)h_7] \quad (3)$$

$$\dot{m}_a = \frac{\dot{Q}_{cooling}}{h_1 - h_3} \quad (4)$$

Similar mass and energy balances were performed for the air-water heat exchanger, membrane evaporative cooler and outdoor membrane humidifier. To provide closure to the model, the closest approach temperature (CAT) and the closest approach pressure (CAP) were defined. The CAT is a design variable that constrains the minimum temperature difference between two streams in a heat exchanger (Equation 5). The CAT was set to be 5°C after performing a parametric analysis on how it affects the system COP and heat exchanger size. Similarly, the CAP is set to be 0.5 kPa to ensure that water vapor pressure at the vacuum pump exit is higher than the partial pressure at state point 12, while maintain reasonable component size and system COP at the baseline condition.

$$T_6 = T_3 - CAT \quad (5)$$

$$P_{v10} = P_{v12} + CAP \tag{6}$$

After defining all state points in the EES model, the overall mass transfer coefficients (*KA*) of the membrane devices were evaluated using the vapor molar flowrate and the logarithmic partial pressure difference method as shown below:

$$\dot{n}_v = KA\Delta P_{V_{LM}} \tag{7}$$

$$\omega_i = 0.622 \frac{P_{v,i}}{P_i - P_{v,i}} \tag{8}$$

Performing this calculations yielded the mass transfer coefficient, *KA*, for the membrane dehumidifier, membrane evaporative cooler and membrane humidifier. These *KA* values are a surrogate for the size of the heat and mass exchanger. Similarly the *UA* of the heat exchanger was calculated using the logarithmic temperature difference and sensible load.

$$\dot{Q}_{HX3} = UA\Delta T_{LM} \tag{9}$$

$$\dot{Q}_{HX3} = \dot{m}_w(h_4 - h_6) \tag{10}$$

$$\dot{Q}_{HX3} = \dot{m}_a(h_2 - h_3) \tag{11}$$

As for the work done by the vacuum pump, it was calculated using the vapor flowrate and the change in enthalpy between the inlet and outlet of the pump as shown in Equation (12), accounting for the assumed isentropic efficiency. Lastly, the indoor air flow rate ($\dot{V}$) was obtained by dividing the total mass flow rate of the air at state point 1 by its density, as shown in Equation (13).

$$\dot{W}_{pump} = \dot{m}_v(h_{10} - h_9) \tag{12}$$

$$\dot{V} = \frac{\dot{m}_1}{\rho_1} \tag{13}$$

All of these equations and balances in this section were solved iteratively in EES to obtain results that satisfies the target design conditions for the membrane system. The results are summarized in the Table 2 below, and will be used as inputs to develop the physical model of the membrane heat pump system discussed next section.

Table 2: Simulation model solution from EES

Variable	Value	Unit
$\boldsymbol{KA_1}$	3.45×10^{-4}	kmol s^{-1} kPa^{-1}
$\boldsymbol{KA_2}$	3.95×10^{-7}	kmol s^{-1} kPa^{-1}
$\boldsymbol{UA_{HX3}}$	0.506	kW K^{-1}
$\boldsymbol{KA_4}$	2.95×10^{-4}	kmol s^{-1} kPa^{-1}
$\boldsymbol{\dot{V}_{indoor}}$	565	ft^3 min^{-1}
$\boldsymbol{\dot{W}_{pump}}$	1.9	kW

2.4 Fixed Physical Model

The individual component mass and transfer coefficients calculated in the previous section of this study were used as inputs in another model, the fixed physical model, in EES. This fixed physical model solve the thermodynamic cycle using the same mass and energy balances as the previous section, except it uses the results highlighted in Table 2 as inputs instead of the design conditions values. The values for $\epsilon_{dehumidifer}$, CAT, CAP, T_{supply}, $\dot{Q}_{cooling}$, and Z were all substituted by the simulation model result values for KA_1, KA_2, UA_3, KA_4, CFM_{indoor} and $\dot{W}_{pump}$ respectively. The COP and EER of the membrane heat pump system is then evaluated using Equations (14) and (15).

$$COP = \frac{\dot{Q}_{cooling}}{\dot{W}_{total}} \tag{14}$$

$$EER = \frac{\dot{Q}_{cooling}\,(Btu\ hr^{-1})}{\dot{W}_{total}\,(W)} \tag{15}$$

The physical model is then used to study the system performance at different ambient conditions / climate zones and lastly compare the system against vapor compression system.

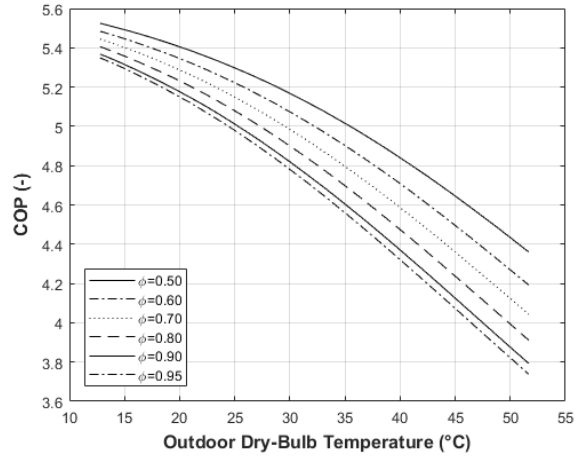

Figure 2: Membrane system COP versus dry-bulb temperature at different relative humidity

3. MODEL ANALYSIS

3.1 Fixed Physical Model Analysis

In this section, parametric analysis were performed using the membrane physical model. Performance parameters such as COP and cooling loads at different indoor and outdoor conditions are evaluated, as well as the conditioned supply air temperature and humidity. The first parametric analysis performed in EES was to evaluate the system performance at different relative humidity levels and outdoor dry-bulb temperatures. The results are shown in Figure 2. For a given dry-bulb temperature, the system COP decreases as relative humidity increases. At high relative humidity, the ambient partial vapor pressure increases, increasing the pressure ratio across the vacuum pump and decreasing the cooling capacity. The COP decreases at fixed relative humidity as dry-bulb temperature increases for similar reasons. For this particular membrane system, the COP is always higher than 4.5 when the ambient dry-bulb temperature is less than 35°C (95°F) for all values of ϕ. This shows that the system is capable of performing effectively in hot humid climates with acceptable COP.

Figure 3 shows the total, latent and sensible loads at two different outdoor dry-bulb temperatures as a function of relative humidity was varied from 0.1 to 0.9 for two outdoor dry-bulb temperatures. Indoor supply air conditions are fixed according to Table 1. Figure 3 shows that the membrane heat pump system latent cooling load decreases with increasing ambient relative humidity and dry-bulb temperature, while the sensible load is relatively unchanged. As the outdoor air humidity ratio increases, the required pressure ratio across the vacuum pump increases. This decreases

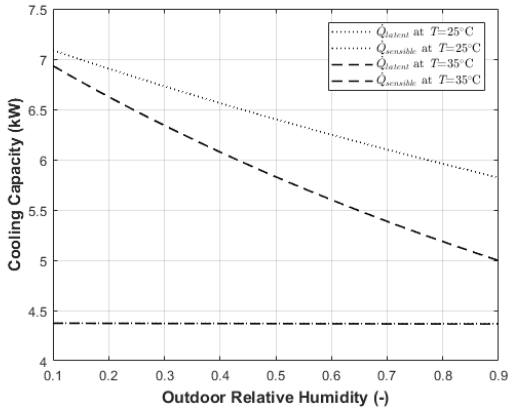

Figure 3: Membrane system cooling loads evaluated at different outdoor conditions

the effectiveness of the membrane dehumidifier, decreasing latent load, while the indirect evaporative cooler performance is not as negatively affected, as the driving pressure difference is much larger.

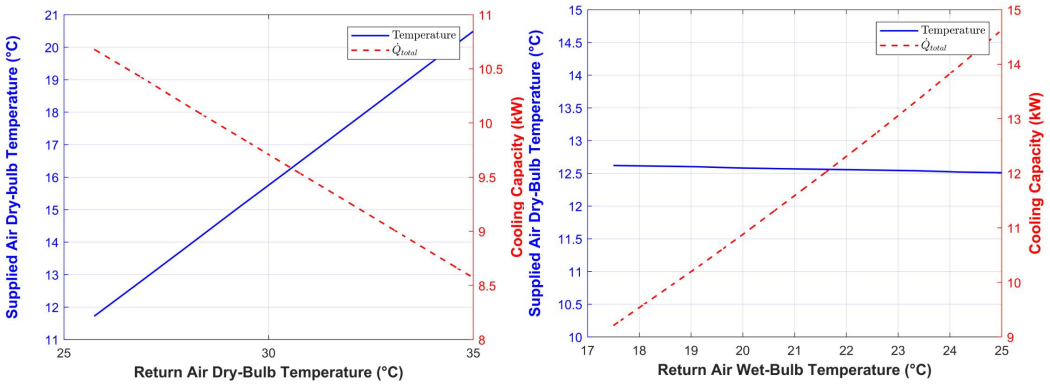

Figure 4: (a) Supplied air dry-bulb temperature at varied return air dry-bulb temperatures, (b) Supplied air dry-bulb temperature at varied return air wet-bulb temperatures

The last study performed for the physical model is to evaluate the supplied air temperature and total cooling load when the indoor unit return dry-bulb and wet-bulb are varied from the standard rating conditions. The results are shown in Figure (4a) and (4b). Figure 4a shows that the supplied air dry-bulb temperature increases as the return dry-bulb temperature increases (with fixed return wet-bulb at 19.4°C, while the provided cooling load decreases. This is because the membrane system model was developed to remove approximately the same amount of sensible heat regardless of the indoor temperature, due to the fixed size of the sensible cooling coil. Therefore, when hotter air passes through the air-water coil the air is cooled down the same amount which results in warmer supplied air temperature. The same reasoning can be used to explain the decrease in the cooling load provided. Interestingly, Figure 4b shows that the system provides more cooling with higher wet-bulb temperatures when the dry-bulb temperature is fixed at the rating condition, T=26.7°C. That is because a higher wet-bulb results in higher humidity, hence a larger partial pressure difference across the vacuum dehumidification device and more latent heat is removed, resulting in a larger cooling capacity by the system.

3.2 Membrane System Performance in Different Climates

One of the objectives of this study is to evaluate the membrane heat pump system performance in different climate regions in the US. To accomplish this, a representative 2000 square foot building was specified in the building energy modeling software eQUEST (DOE, 2017). The hourly cooling load for the building was predicted for 10 different cities in 6 climate zones within the United States. The 10 cities that were chosen for this study are: Atlanta, Chicago, Houston, Los Angeles, Madison, WI, Miami, Minneapolis, Phoenix, Portland, OR and Washington D.C. For each

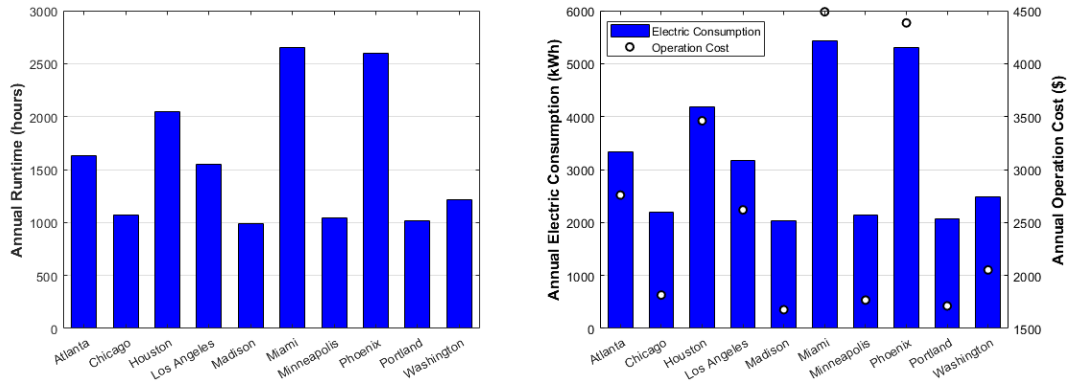

Figure 5: (a) Membrane system annual runtime, (b) Membrane system annual electric consumption and operation costs

hour of the year and for each location, the COP, EER, sensible and latent heat and total cooling capacity of the membrane system were simulated with the physical model described above using the hourly ambient dry-bulb and wet-bulb as inputs, and assuming ASHRAE indoor rating conditions. The total system run time and related electric were calculated by dividing the hourly building load from eQUEST by the predicted total cooling load from EES for that hour. The annual runtime for each city is presented in Figure 5a below. As expected, Miami which generally has a hot and humid climate had the maximum hours of operations at 2657 hr, whereas Madison which is colder had the least at 992 hr. In addition to the runtime required, the annual electric consumption for each city, as well as the cost using the average electric rate for each city (EIA, 2018) is reported in Figure 5b.

Although the runtime and electric consumption varying from one climate to another, the membrane heat pump system had a relatively stable performance values in all climate zones. Table 3 below compares the system annual average performance parameters for five of the cities. This comparison shows the capability of the system to perform in different climate zones.

Table 3: Annual averaged performance values of the membrane system in different climate zones

	Atlanta	**Chicago**	**DC**	**Madison**	**Miami**
COP	5.36	5.46	5.41	5.48	5.14
EER	18.29	18.64	18.46	18.70	17.55
Total cooling load	10.90	11.10	11.00	11.14	10.46
Supplied air dry-bulb temperature (°C)	12.60	12.60	12.60	12.56	12.62
Supplied air relative humidity	0.31	0.28	0.30	0.28	0.37

3.3 Comparison with Vapor Compression Systems

In this section, the membrane heat pump system is compared to conventional vapor compression systems. Performance parameters, such as the COP and the total cooling provided, are compared to two commercially available vapor compression systems with heat pumps, with seasonal energy efficiency ratio (SEER) values of 14 and 16 and cooling capacity of 3 tons. The vapor compression curves was generated from the available technical specifications from a heat pump manufacturer (Goodman, 2018a, 2018b). Figures 6a and 6b shows how the membrane system COP compared with the vapor compression systems at different outdoor dry-bulb temperatures. The membrane heat pump is much less sensitive to outdoor ambient than the vapor compression systems. The COP of the membrane heat pump system was higher than 4.5 for the entire range of outdoor dry-bulb temperature, from 25°C to 50°C, whereas the vapor compression system COP studied decreased drastically from 5 to 2.3, which is approximately a 50% drop at the same outdoor temperature range. The difference in the COP sensitivity to outdoor temperatures for the two HVAC systems is significant and is due to the differences of their cooling processes. The membrane heat pump system, however, is more sensitive to the indoor supply air conditions compared to the vapor compression system. A change of 2.8°F in the indoor unit supply dry-bulb temperature decreases the membrane system's COP by 0.3, whereas it barely decreases the vapor compression system COP. Another comparison that shows the membrane system sensitivity to the indoor unit's conditions is presented in Figure 7a. The indoor unit supply air dry-bulb temperature was kept

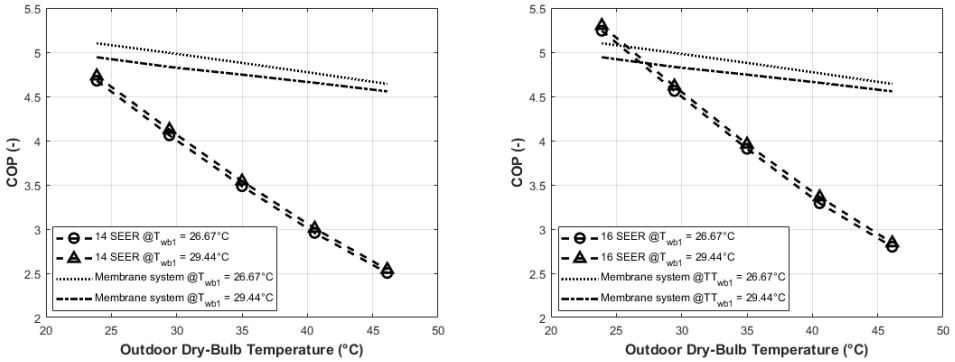

Figure 6: (a) Comparison between the membrane system and 14 SEER vapor compression system, (b) Comparison between the membrane system and 16 SEER vapor compression system

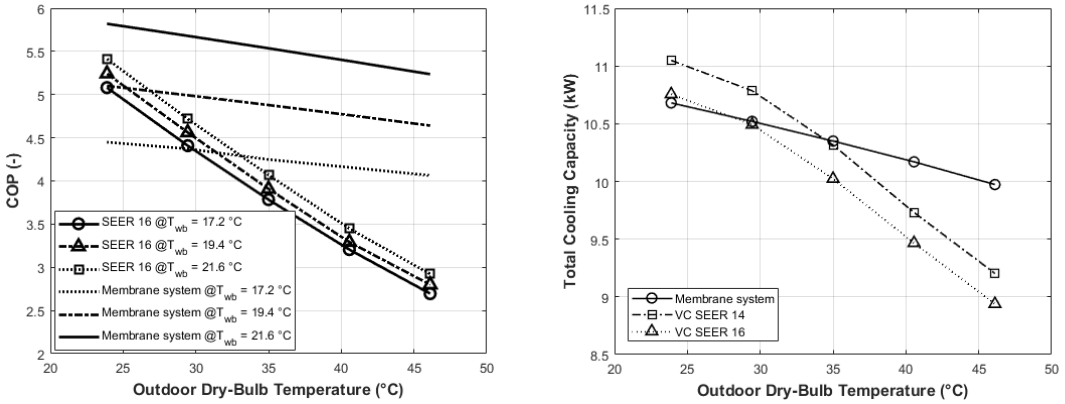

Figure 7: (a) Indoor unit's wet-bulb temperature effect on system's COP (b) Total cooling load provided by the 3 systems at different outdoor dry-bulb temperature

constant at the rating condition, 26.67°C (80°F), and the COP was evaluated for both systems at indoor wet-bulb temperatures of 17.2°C (63°F), 19.4°C (67°F) and 21.67°C (71°F). These 3 values were chosen following the available performance data for the vapor compression system. An increase in the indoor wet-bulb temperature increases both systems COP, however only the membrane system benefit from it significantly. Varying the wet-bulb from 17.2°C to 21.6°C, increased the membrane system's COP by 35%, and increases the vapor compression's COP by 7%. An increase in the indoor wet-bulb results in more humidity, hence, more latent heat can be removed by the membrane system providing more overall cooling load which explains the increased COP. Lastly, the total cooling capacity of the three systems are compared. The cooling loads are evaluated at the same outdoor temperature range as the previous graphs. Figure 7b illustrates the three system's cooling capacities. The results in Figure 7b are consistent with those shown in previous plots, the membrane system's cooling load does not drop significantly over the outdoor dry-bulb temperature range compared to the vapor compression systems. The membrane system generally provides less cooling compared to the vapor compression system, however, it is more stable for a larger temperature range, giving the system an advantage over the compression systems for performing through the different seasons of the year.

4. CONCLUSIONS

The membrane heat pump systems investigation shows potential as an alternative to vapor compression systems as the performance are more stable at wide range of outdoor temperatures while maintaining relatively high COP and EER at different climate zones. This results in significant energy savings compared to compression systems while also being environmentally friendly as water is the only fluid used by the system. However, membrane systems require makeup water to be supplied. In addition, development of an efficient vacuum pump that can manage the pressure ratio and required volumetric flow rate is critical. Like in vapor compression systems, the compressor is the critical component in achieving theoretical efficiency targets.

NOMENCLATURE

COP	cost of performance	(-)
EER	energy efficiency ratio	(Btu W^{-1} hr^{-1})
h	specific enthalpy	(kJ kg^{-1})
KA	mass transfer coefficient	(kmol s^{-1} kPa^{-1})
$\dot{m}$	mass flowrate	(kg s^{-1})
$\dot{n}$	molar flowrate	(kmol s^{-1})
P	pressure	(kPa)
$\dot{Q}$	cooling load	(kW)
T	temperature	(°C)

UA	heat transfer coefficient	(kW K^{-1})
$\dot{V}$	volumetric air flowrate	(ft^3 min^{-1})
$\dot{W}$	work done	(kW)

Greek letters

ω	humidity ratio	(-)
ϵ	dehumidifier effectiveness	(-)
ρ	density	(kg m^{-3})

Subscript

v	vapor
a	air
LM	logarithmic mean
1, 2, etc.	State point number

REFERENCES

ASHRAE. (2017). *2017 ASHRAE Handbook - Fundamentals*. Atlanta, GA: ASHRAE.

Department of Energy, (2017), viewed January 2017, URL http://www.doe2.com/equest

EIA. (2013). Heating and cooling no longer majority of U.S. home energy use. Retrieved March 1, 2018, from https://www.eia.gov/todayinenergy/detail.php?id=10271

EIA. (2018). US. Energy Information Administration - State Electricity Profiles. Retrieved March 3, 2018, from https://www.eia.gov/electricity/state/

Goetzler, W., Zogg, R., Young, J., & Johnson, C. (2014a). Alternatives to HVAC Technology. *ASHRAE Journal*, (October), 12–23.

Goetzler, W., Zogg, R., Young, J., & Johnson, C. (2014b). *Energy Savings Potential and R&D Opportunities for Non- Vapor-Compression HVAC*. Burlintgon, MA. Retrieved from http://energy.gov/sites/prod/files/2014/03/f12/Non-Vapor Compression HVAC Report.pdf

Goodman. (2018a). GSZ14 Heat Pump. Retrieved March 1, 2018, from https://www.goodmanmfg.com/products/heat-pumps/14-seer-gsz14

Goodman. (2018b). GSZ16 Heat Pump. Retrieved March 1, 2018, from https://www.goodmanmfg.com/products/heat-pumps/16-seer-gsz16

Klein, S. A. (2017). Engineering Equation Solver. Madison, WI: F-Chart Software.